Materials Science-Poland, *Vol. 27*, *No. 4/1*, *2009*

The effect of hydrothermal temperature on the synthesis of monoclinic bismuth vanadate powders

A. ZHANG*, J. ZHANG

College of Sciences, North China University of Technology, Beijing 100144, P.R. China

Pure phase monoclinic bismuth vanadate powders of a nanosized diameter were synthesized by the hydrothermal method and characterized using XRD, TEM, DRS, Raman and FTIR techniques. The results revealed that the hydrothermal conditions (16 h at 140–240 °C) are favourable for the formation of monoclinic bismuth vanadate powders. They also indicated that if samples are prepared by the route described in this paper, an increase in the grain size and a gradual decrease of the band gap occur as the hydrothermal temperature increases.

Key words: *bismuth vanadate; hydrothermal method; hydrothermal temperature*

1. Introduction

The photocatalytic degradation of organic and inorganic pollutants involves reactions that offer much promise for the solution of urgent environmental issues that confront mankind today. Great progress has been made in the research and application of these reactions, mostly with semiconductors under UV light irradiation [1, 2]. Presently, developing visible light responsive photocatalysts is the most important research direction in this field, because the utilization of visible light, which accounts for more than half of the solar spectrum, is significant. However, most of the photocatalysts developed thus far have wide band gaps, and can therefore utilize only a very small portion of sunlight. Only a limited number of photocatalysts absorbing visible light have been discovered so far [3, 4].

Bismuth vanadate ($BiVO_4$) has recently attracted considerable attention for its strong photocatalytic effect on water splitting and pollutant degradation under visible light irradiation [5–7]. There are three crystalline phases reported for synthetic $BiVO_4$, namely the monoclinic scheelite type, the tetragonal sheelite-type and the tetragonal zircon type and the photocatalytic properties are strongly influenced by its crystal

*Corresponding author, e-mail: a.p.zhangg@gmail.com)

phase. The phase transition between monoclinic scheelite structure and tetragonal scheelite structure of $BiVO_4$ reversibly occurs at about 255 °C, whereas the irreversible transition from tetragonal zircon structure to monoclinic $BiVO_4$ occurs after heat treatment at 400–500 °C and cooling to room temperature [8].

Since the first fabrication of crystalline $BiVO_4$, several methods have been reported for the preparation of $BiVO_4$ such as solid state reaction, the sol–gel method, the hydrothermal method, coprecipitation, metalorganic decomposition, etc. Hydrothermal synthesis, a soft chemical process depending upon many factors such as the hydrothermal treatment, pH, temperature and duration of synthesis, etc., can be used to fabricate materials with various morphologies and photocatalytic properties [9–12]. This study reports on a hydrothermal route for the synthesis of pure phase monoclinic $BiVO_4$ powders. For comparison, various temperatures were used, and all samples were characterized by X-ray diffraction (XRD), transmission electron microscopy (TEM), diffuse reflectance spectra (DRS), Raman and FTIR techniques.

2. Experimental

Materials and process. Bismuth nitrate pentahydrate ($Bi(NO_3)_3{\cdot}5H_2O$, analytical grade) and ammonium metavanadate (NH_4VO_3, analytical grade) from Beijing Chemical Company were used as received without further purification. All other chemicals used in the experiments were also analytical grade reagents, and deionized water was used for preparation of solutions.

In a typical preparation process, 0.02 mol $Bi(NO_3)_3{\cdot}5H_2O$ and 0.02 mol NH_4VO_3 were dissolved in 20 cm^3 of 65% (w/w) HNO_3 and 20 cm^3 6 M NaOH solutions separately, and each stirred for 2 h at room temperature. After that, these two mixtures were mixed together and stirred for about 1 h to get a stable, salmon-pink, homogeneous mixture. Then, the mixture was sealed in a 50 cm^3 Teflon-lined stainless autoclave, and allowed to heat for 16 h at hydrothermal temperatures ranging from 140 to 240 °C under autogenous pressure in an oven. Finally, the precipitate was filtered, washed three times with distilled water, and dried in vacuum at 80 °C for 12 h.

Characterization. X-ray powder diffraction (XRD, Beijing Purkinjl General Instrument Co. LTD, model XD-3; accelerating voltage 36 kV, applied current 30 mA) patterns were recorded in the region of 2θ from 17° to 55° using $CuKi_\alpha$ radiation (λ = 0.15418 nm) with a step scan of 4.0 deg/min at room temperature using a counter diffractometer (graphite monochromator, proportional counter). The morphologies and particle sizes of samples were examined by transmission electron microscopy (TEM, Hitachi Model H-7500; accelerating voltage 80 kV). Before placement onto Cu netting for TEM preparation, the samples were all dispersed in anhydrous ethanol: water 1: 1 solution (V/V) and treated in ultrasonic cleaner for each about 2 min. The Raman spectra were recorded by a microprobe Raman system (Renishaw H13325 spectrophotometer) with a holographic notch filter and a CCD detector, and the excitation at 514.5 nm (12 MW at the head) from an Ar ion laser. All the samples were oriented on

the stageof an Olympus BHSM microscope, equipped with 15× and 50× objectives, and recorded at the resolution of 2 cm^{-1} in the range from 150 to 1000 cm^{-1}. The FTIR spectra were recorded at RT using a Perkin-Elmer spectrometer (model Gx) with Spectrum Gx software Kit (Issue B). All the FTIR transmittance spectra of samples that had been pressed into KBr pellets were collected in the wave number range from 400 to 1800 cm^{-1} using the KBr beam splitter. Optical absorption spectra of the samples were obtained on a doubled-beam UV-visible spectrophotometer (model YU-1901, Beijing Purkinjl General Instrument Co. LTD) equipped with an integrating sphere. UV-vis diffuse reflectance spectra (DRS) of $BiVO_4$ were recorded by using $BaSO_4$ as a reference, and were converted from reflection to absorbance by the Kubelka–Munk method [13].

3. Results and discussion

3.1. XRD results of $BiVO_4$ powders

Figure 1 shows the XRD patterns of samples prepared for 16 h at various hydrothermal temperatures. It is clear that these diffraction peaks are all in good agreement with the standard Joint Committee on Powder Diffraction Standards (JCPDS) card No. 14-0688, which is assigned to monoclinic $BiVO_4$. No impurity peaks were observed in any of these XRD patterns.

The results indicate that the hydrothermal conditions imposed (hydrothermal synthesis for 16 h over a wide range of temperatures) are favourable for the formation of monoclinic scheelite $BiVO_4$.

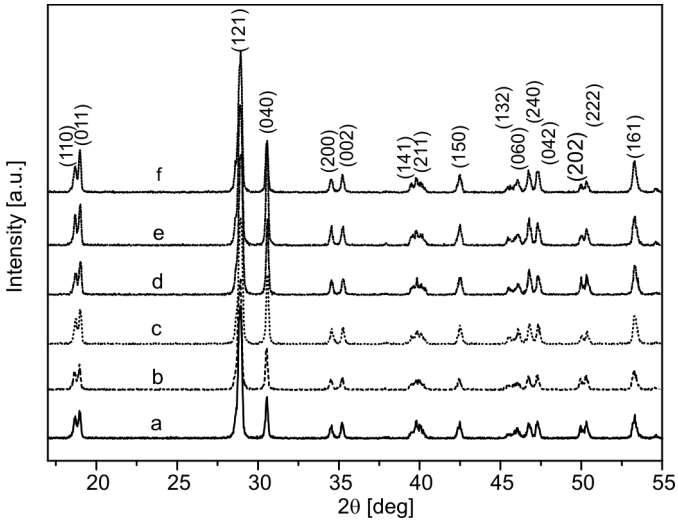

Fig. 1. XRD patterns of $BiVO_4$ prepared at various hydrothermal temperatures T [°C]: a) 140, b) 160, c) 180, d) 200, e) 220, f) 240

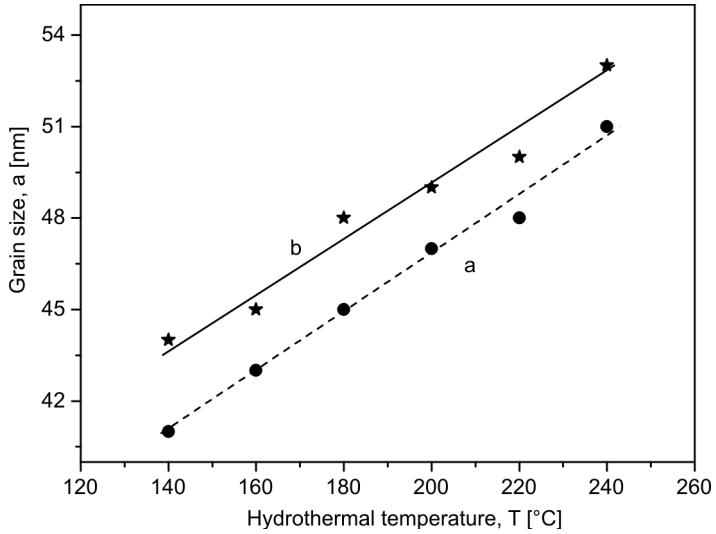

Fig. 2. The dependence of the grain size on the hydrothermal temperature:
a) calculated from the Scherrer formula with XRD results,
b) calculated according to the statistical analysis of large number (100–150)
of particles from TEM pictures

The crystalline size of these powders was estimated from the Scherrer formula [14]

$$D = \frac{K\lambda}{\sqrt{\beta_s^2 - \beta_e^2}\cos\theta} \tag{1}$$

where D is the crystal size, K is usually taken as 0.89 [5, 12, 14]; λ is the wavelength of the X-ray radiation (0.15418 nm); β_s and β_e are the peak widths at half-maximum height of the sample and the equipment broadening, respectively; $2\theta = 30.55°$ as for monoclinic $BiVO_4$ [5, 12]. As a result, the crystal sizes of samples were evaluated as 41, 43, 45, 47, 48, 51 nm for samples (a) to (f) respectively, showing a clear growth trend, as can be seen from line *a* in Fig. 2.

3.2. TEM results for $BiVO_4$ powders

Figure 3 shows TEM images of $BiVO_4$ powders and their relative abundance of particles prepared at various temperatures. It shows that all primary particles with nanosized diameters were relatively similar in size and were almost spherical. Particle sizes and their relative abundance were estimated according to the statistical tests for a large number (100–150) of particles, and the average diameters of particles were measured as 44, 45, 48, 49, 50, 53 nm in Fig. 3af, respectively. It revealed that phase-pure monoclinic $BiVO_4$ with nanosized diameter can be synthesized effectively by the hydrothermal method.

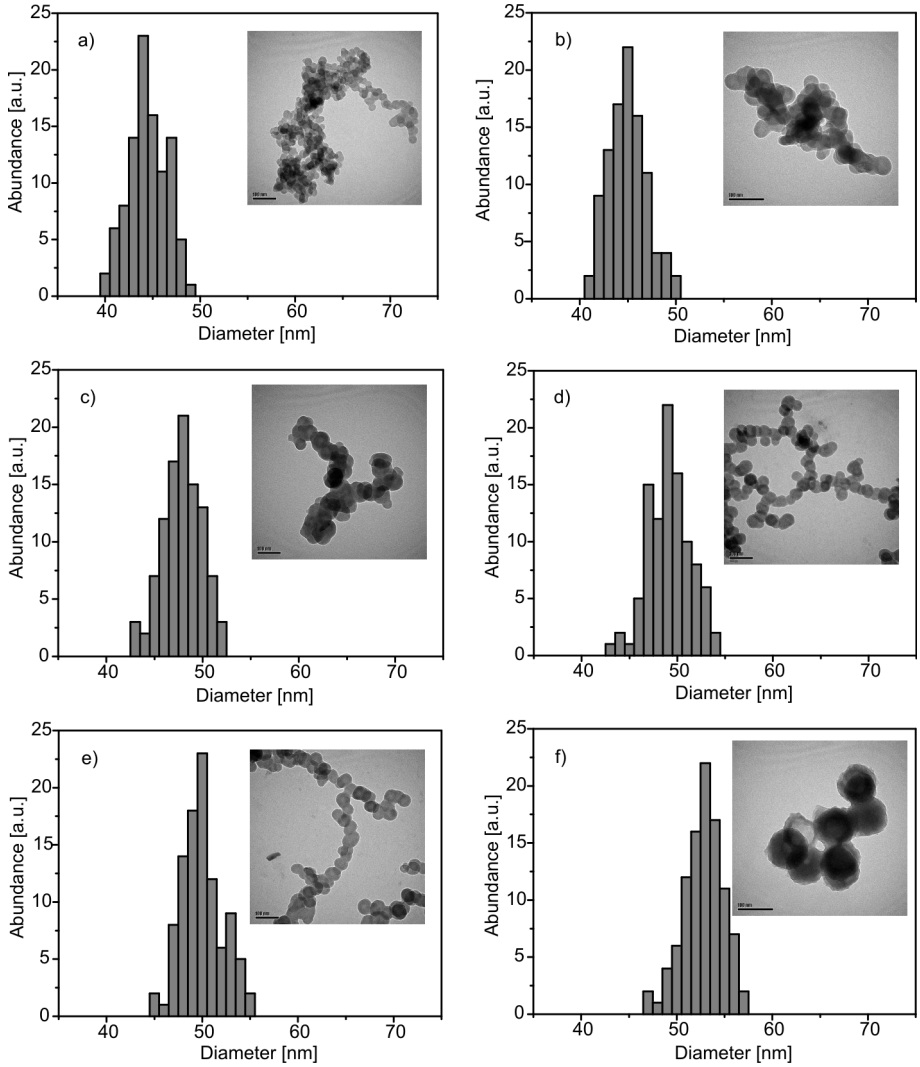

Fig. 3. TEM images of $BiVO_4$ and their relative abundance of grain size fabricated at various hydrothermal temperatures, T [°C]: a) 140, b) 160, c) 180, d) 200, e) 220, f) 240

It is clearly seen from TEM data that linear-chain aggregations of particles occur. These aggregations might be formed by the sintering of nanosized particles in the long duration process of synthesis, because many single nanoparticles were also observed. Furthermore, the $BiVO_4$ sample prepared at low temperature has even more particle aggregation (Fig. 3a), and each aggregation looks agglomeration-like, with an asymmetrical shape measuring about ten times the particle size. When prepared at high temperature, samples with a nearly spherical form are obtained (Fig. 3f) and the average particle size is greater than that obtained at low temperature, showing a growth trend as a function of increasing temperature, as seen in Fig. 2, line b. It is

interesting that the average particle size and the associated, temperature-dependent growth trend are in good agreement with their expected values according to the Scherrer equation based on XRD patterns; furthermore, some of the larger particle sizes observed in TEM pictures may be attributed to minor anomalies in the implementation of experiments

3.3. Raman and FTIR results for $BiVO_4$ powders

The Raman spectra of the 150–1000 cm^{-1} region of samples are shown in Fig. 4a. The results of the band component analysis [15, 16] of Raman and IR spectra of sam

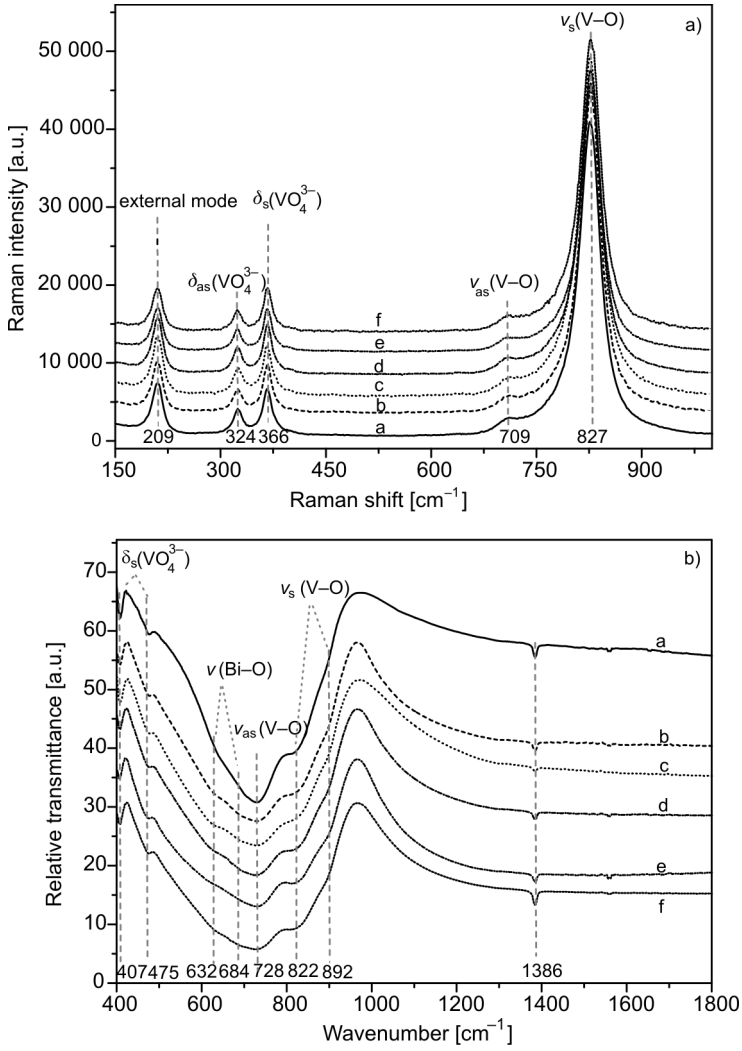

Fig. 4. Raman (a) and FTIR (b) spectra of $BiVO_4$ fabricated at various hydrothermal temperatures, T [°C]: a) 140, b) 160, c) 180, d) 200, e) 220, f) 240

ples are also marked in Fig. 4. It showed the same feature, namely that each spectrum was dominated by an intense Raman band at 827 cm^{-1} assigned to ν_s(V–O), and with a weak shoulder at about 709 cm^{-1} assigned to ν_{as}(V–O). The $\delta_s(VO_4^{3-})$ and $\delta_{as}(VO_4^{3-})$ modes are at 366 and 324 cm^{-1}, respectively, and external modes (rotation/translation) occur at 209 cm^{-1}. Figure 4b shows FTIR spectra of recorded samples, ranging from 400 to 1200 cm^{-1} at RT. All the samples are mainly characterized by a broad and strong IR band near 728 cm^{-1} with shoulders at 892, 822, 684 and 632 cm^{-1}. One weak CO_3^- derived band is observed at 1386 cm^{-1}, which might be due to the adsorption of atmospheric carbon dioxide during the experiments [15, 17]. It reveals that all the samples exhibited the same monoclinic scheelite structure, although their particle diameters and particle morphologies increased in a continuous manner as the hydrothermal temperature increased from 140 to 240 °C.

3.4. DRS results of $BiVO_4$ powders

It is well known that the electronic structure of the semiconductor usually plays a crucial role in its photocatalytic activity [14, 18]. DFT calculations of the electronic structure [19] showed that the valence band (VB) of $BiVO_4$ is composed of hybridized Bi 6s and O 2p orbitals, whereas the conduction band (CB) is composed of V 3d orbitals; and the hybridization of the Bi 6s and O 2p orbital may enhance the migration of photo-excited holes, which is beneficial to photocatalytic oxidation of organic pollutants [5, 7, 20].

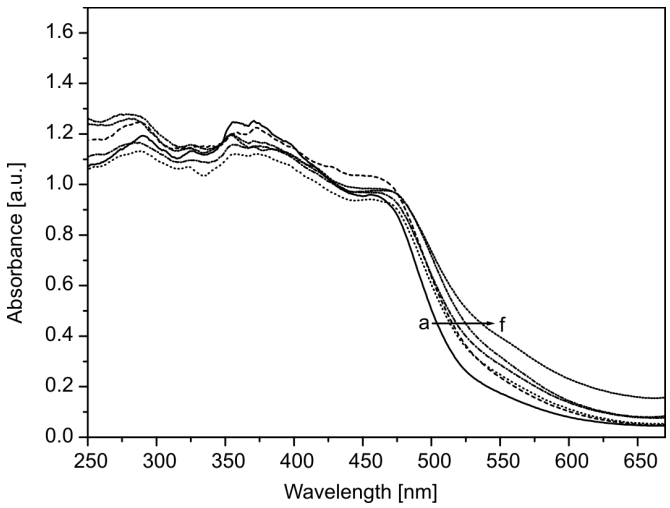

Fig. 5. DRS spectra of $BiVO_4$ fabricated at various hydrothermal temperatures, T [°C]: a) 140, b) 160, c) 180, d) 200, e) 220, f) 240

Figure 5 shows the DRS of $BiVO_4$ prepared hydrothermally at various temperatures. It was found that all samples showed strong absorption in the visible light re-

gion, in addition to that in the UV region, which is the characteristic absorption profile of monoclinic scheelite $BiVO_4$. The steep gradients of spectra indicated that the visible light absorption is due to the band-gap transition, and the prolonged absorption tail, up to about 650 nm, should result from the crystal defects that form when $BiVO_4$ grows [5, 9]. The absorption edges of samples shift to red, from about 530 to 590 nm, as the hydrothermal temperature increases, which indicates different band gaps of the samples. As in a crystalline semiconductor, the band gaps can be calculated from the following equation [12, 21],

$$\alpha h\nu = A\left(h\upsilon - E_g\right)^{n/2} \tag{2}$$

where α, ν, E_g and A are the absorption coefficient, incident light frequency, band gap and a constant, respectively. Among them, n depends on the characteristics of the transition in a semiconductor, i.e., direct transition (n = 1) or indirect transition (n = 4). For $BiVO_4$, n is taken as 1 [12, 15]. The band gap energy for the $BiVO_4$ can be thus estimated from a plot $(\alpha h\nu)^2$ versus photon energy ($h\nu$), as can be seen from Fig. 6.

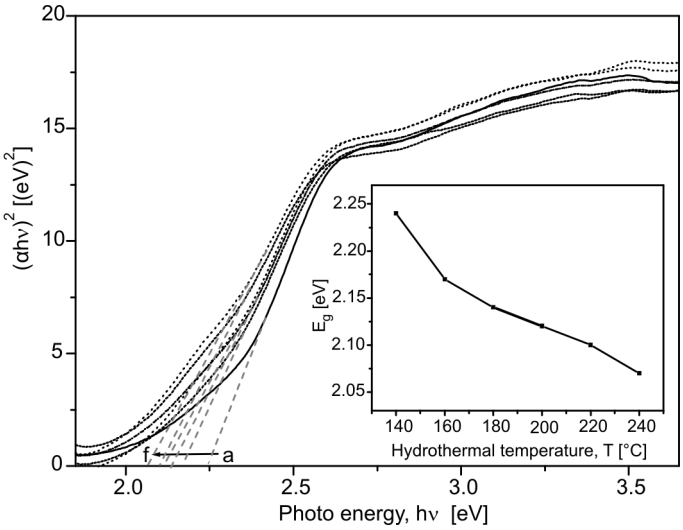

Fig. 6. Plots of the $(\alpha h\nu)^2$ versus photo energy ($h\nu$) for $BiVO_4$ powders fabricated at various hydrothermal temperatures, T [°C]: a) 140, b) 160, c) 180, d) 200, e) 220, f) 240

The intercept of the tangent to the x axis will give a good approximation of the band gap for $BiVO_4$. Thus the E_g of $BiVO_4$ can be estimated about 2.24, 2.17, 2.14, 2.12, 2.10 and 2.07 eV for samples (a)–(f) respectively, showing a decreasing trend, as can be seen in the inset of Fig. 6. These data clearly demonstrate that the electronic structures of $BiVO_4$ were changed by the temperature used in the hydrothermal synthesis. It proves that the variations in the hydrothermal temperature led to different degrees of aggregation and changes of grain size, which therefore resulted in the samples having different electronic structures.

4. Conclusion

Highly crystallized monoclinic $BiVO_4$ crystals with nanosized diameters were synthesized hydrothermally and characterized by XRD, TEM, DRS, Raman and FTIR techniques. From XRD and TEM data, the grain size was observed to increase when the hydrothermal temperature increased from 140 to 240 °C. DRS results indicated that samples prepared at higher hydrothermal temperatures may consist of larger particles with less aggregation, and thus lead to a smaller band gap.

Acknowledgement

We acknowledge the financial support of the Scientific Research Foundation of North China University of Technology and the Natural Science Foundation of Beijing. Professor Y. Fang (Capital Normal University, P.R. China) and Miss Q. Cheng (Beijing Purkinjl General Instrument Co. LTD, P.R. China) are also thanked for conducting tests and for helpful discussions regarding this manuscript.

Reference

[1] FUJISIMA A., HONDA K., Nature, 37 (1972), 238.
[2] FUJISHIMA A., RAO T.N., TRYK D.A., J. Photochem. Photobiol. C, 1 (2000), 1.
[3] KUDO A., UEDA K., KATO H., MIKAMI I., Catal. Lett., 53 (1998), 229.
[4] KOHTAIN S., HIRO J., YAMAMOTO N., KUDO A., TOKUMURA K., NAKAGAKI R., Catal. Commum., 6 (2005), 185.
[5] YU J.Q., KUDO A., Adv. Funct. Mater., 16 (2006), 2163.
[6] KOHTANI S., KOSHIKO M., KUDO A., Appl. Catal. B: Environ., 46 (2003), 573.
[7] TUCKS A., BECK H.P., Dyes Pigments, 72 (2007), 163.
[8] KUDO A., OMORI K., KATO H., J. Am. Chem. Soc., 121 (1999), 11459.
[9] YAO W.F., YE J.H., Chem. Phys. Lett., 450 (2008), 370.
[10] ZHOU L., WANG W.Z., XU H.L., Cryst. Growth Des., 8 (2008), 728.
[11] ZHANG L., CHEN D.R., JIAO S.X., J. Phys. Chem. B, 110 (2006), 2668.
[12] ZHANG X., AI Z.H., JIA F.L., ZHANG L.Z., FAN X.X., ZOU Z.G., Mater. Chem. Phys., 103 (2007), 162.
[13] KUBELKA P., MUNK F.E., BEITRAG O.F., Z. Tech. Phys., 12 (1931), 593.
[14] WELLER M.T., *Inorganic Materials Chemistry*, Oxford University Press, London, 1994.
[15] LIU J.B., WANG H., WANG S., YAN H., Mater. Sci. Eng. B, 104 (2003), 36.
[16] GOTIĆ M., MUSIĆ S., IVANDA M., ŠOUFEK M., POPOVIĆ S., J. Mol. Struct., 744–747 (2005), 535.
[17] GALEMBECK A., ALVES O.L., J. Mater. Sci., 37 (2002), 1923.
[18] FU H., PAN C., YAO W., ZHU Y., J. Phys. Chem. B, 109 (2005), 22432.
[19] OSHIKIRI M., BOERO M., YE J., ZOU Z., KIDO G., J. Chem. Phys., 117 (2002), 7313.
[20] TANG J., ZOU Z.G., YE J.H., Angew. Chem. Int. Edit., 43 (2004), 4463.
[21] BUTLER M.A., J. Appl. Phys., 48 (1977), 1914.

Received 4 July 2008
Revised 3 October 2008